ChemComm

COMMUNICATION

Imaging the Belousov–Zhabotinsky reaction in real time using an ion sensitive array†

Balazs Nemeth,[a] Christoph Busche,[b] Soichiro Tsuda,[c] Leroy Cronin*[b] and David R. S. Cumming*[a]

We show how an array of ion-sensitive-field-effect-transistors can be used to both spatially and temporally image the oscillating pH/ion waves produced by the Belousov–Zhabotinsky (BZ) reaction with high resolution.

Non equilibrium chemistry often displays complex spatial and temporal dynamics, for instance in the example of the BZ reaction in a thin film[1] or in the morphological transformation of polyoxometalate crystals into tubular architectures.[2] Such processes have been well studied[1,2] but the direct spatial and temporal probing of ion fluxes is extremely difficult to achieve.[3] One possible way to image such ion fluxes is by the integration of semiconductor based chemical sensor devices into a sensor array, for example using ion-sensitive field-effect transistors (ISFETs).[4] Indeed, there have been several applications using ISFET devices as chemical sensors for biodiagnostic or for reaction control.[5,6]

Herein we show that it is possible to image the variations in the spatial-temporal ion flux that occurs during the course of the Belousov–Zhabotinsky (BZ) reaction.[7] But the usability of ISFET sensors is not limited to the BZ reaction, which is merely a model for possible use in biological systems.

The BZ reaction belongs to a group of oscillating chemical reactions, first discovered by Belousov in 1950s as a model of biological cyclic reactions, such as the citric acid cycle.[8] This oscillating chemical reaction has been extensively studied in various contexts for example nonlinear dynamical systems[9] and complexity theory.[10] In recent years the BZ reaction has been utilized for unconventional computing systems[11] and in functionalized self-oscillating gels.[12] The self-oscillating BZ reaction, which is observed as intermittent excitation events, has been measured in terms of colour, absorption, and electrical potential so far. However, those measurement systems were able to provide macroscopic information only. To address this issue we utilised an ion sensor array (ISA), which has the sensitivity and the speed required to accurately monitor propagating ion waves of the BZ reaction with high spatial and temporal resolution.

The elementary unit of the system is a pixel that is replicated throughout the sensor array. The schematic design of a pixel circuit and the micrograph of the fabricated system are presented in Fig. 1. Each unit consists of 4 transistors occupying a space of 10.2×10.2 μm. To use CMOS transistors as ISFET sensors connection needs to be established between the floating gate of the CMOS transistor and an ion-sensitive layer through intermediate vias and metal layers (see Fig. 2).
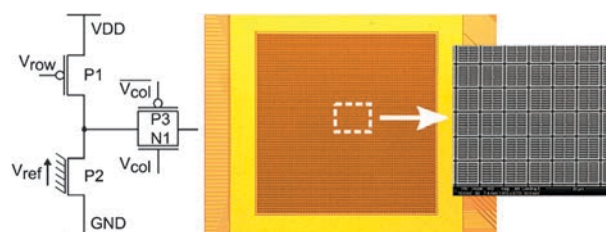
**Fig. 1** Schematic design of the pixel circuit and micrographs of the sensor devices.

The ion-sensitive silicon nitride membrane is directly exposed to liquids on the surface of the semiconductor chip. The solution on the top of the sensor solvates this membrane, forming a double-layer capacitor at the membrane-electrolyte interface. The static and fluctuating potentials that drop across the membrane-electrolyte interface appear at the polysilicon gate of the transistor due to the capacitive coupling between the interface and the top-metal layer. These potentials have therefore direct influence on the channel regions of the ISFET devices (for further details see ESI†). The ISFET device was calibrated with respect to pH-changes. It should be emphasised that the device is in general reacting to a fluctuation of ions.[13] The Si_3N_4 layer on the other side shows the highest sensitivity to changes in pH. The resulting 64×64 array of p-type ISFET based lab-on-a-chip monolithic ion-camera has a response readout of 19.2 mV/pH (see ESI†). Non-nernstian behaviour is known for Si_3N_4 as a result of SiO_2 present in the layer.[14]

[a] *Electronics Design Centre, School of Engineering, University of Glasgow, G12 8LT, UK. E-mail: David.Cumming.2@glasgow.ac.uk; Web: http://www.gla.ac.uk/schools/engineering/staff/davidcumming/*
[b] *WestCHEM, School of Chemistry, University of Glasgow, G12 8QQ, UK. E-mail: Lee.Cronin@glasgow.ac.uk; Web: http://www.croninlab.com*
[c] *Exploratory Research for Advanced Technology (ERATO), Japan Science and Technology Agency, Yamadaoka 1-5, Suita, Osaka 565-0871, Japan. E-mail: tsuda-soichiro@bio.eng.osaka-u.ac.jp*
† Electronic supplementary information (ESI) available. See DOI: 10.1039/c2cc30811h
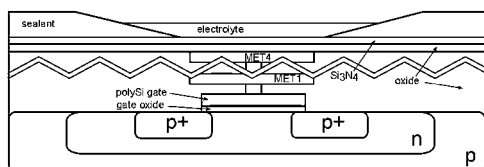
Fig. 2 Simplified cross-sectional representation of a p-type ISFET that follows the standard CMOS structure with oxides, metals and the ion-sensitive silicon nitride layer.

In our experiments one complete readout of the 64 × 64-pixel array takes 17 ms (58 FPS—frame per second) at a sampling rate of 66 µs per pixel. This enabled us to record spontaneous pH fluctuations and the spread of ions during the BZ reaction in real-time. For the actual experiments 5.5 ml samples of the *pre-BZ solution*[15] were mixed with 1 ml of ferroin indicator solution in a plastic container on the top of the ceramic chip carrier. Fig. 3 demonstrates the measured responses of ISFET pixel (27;31) of the reaction over second ranged time scale. In the first 37 s the pre-BZ solution and the ferroin indicator are reacting and the rising trend of the curve indicates that the solution becomes more acidic. The large increase in the value of the pixel output voltage represents the trigger event of the reaction. It is followed by voltage steps with considerable less amplitudes in the expected 30–60 s time intervals.
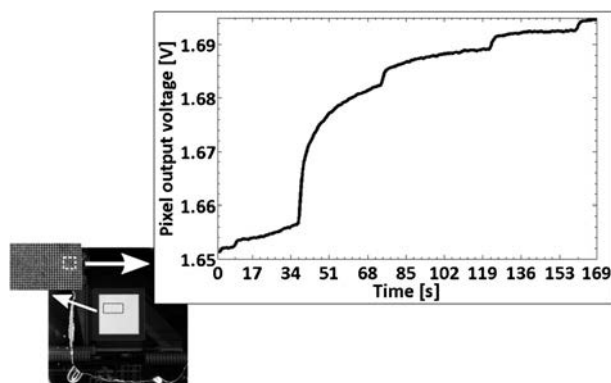

Fig. 3 Output voltage response of pixel (27;31) during the BZ-reaction.

Baseline measurement showed a constant negative trend in the pixel output voltage, thus the elevation of the curve can be clearly attributed to the increasing acidity. Over the selected pixel the reaction triggered at $t = 37$ s with a nonlinear increase in pH. The resulting curve showed a 0.8 pH increase over the course of 10 s. The pH values corresponding to the minor voltage steps are summarized in Table 1.

Table 1 Voltage increase as a function of pH

| Minor voltage steps	Approximated signal rising time [s]	Voltage increase [mV]	ΔpH
1.	2.4	3	0.15
2.	3.5	3	0.15
3.	4.5	1	0.05

The three and two dimensional representations of the H^+ spread induced pixel output voltage distributions are shown in Fig. 4 at time point of 37.4 s.
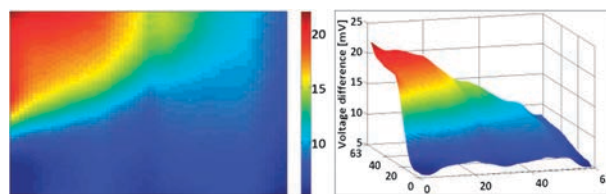

Fig. 4 Three and two dimensional representation of the pH fluctuation induced output voltage difference at 37.4 s, red displays the highest and blue the lowest output potential. The imaged area is 64 × 64 pixel, 715.8 × 715.8 µm. The x–y axis is number of pixels.

A reference data frame was chosen and stored for each data extraction cycle. The values of the reference data frame were systematically subtracted from the values of the actual raw data frame, to give the signals of interest. The images demonstrate the extracted output difference signal at the specified time point that is approximately 400 ms after the first trigger event occurs at pixel (27;31). The results comply with the plotted data in Fig. 3. The trigger events of the BZ reaction were investigated to show the directions of the H^+ ions spreading across the sensor array. It is apparent that the reaction is triggered from the top-left corner of the ISA where the Ag/AgCl reference electrode was located during the measurements. The next voltage steps (1–3 Table 1) were initiated from the same corner as well. Their flow in terms of ionic spread appeared to be similar to the first trigger event. The start of the overall reaction is visualized in Fig. 5 in 2D at time points of 34 s, 35.7 s, 36.8 s, 37.4 s, 39.7 s, 41.1 s and 43.3 s.
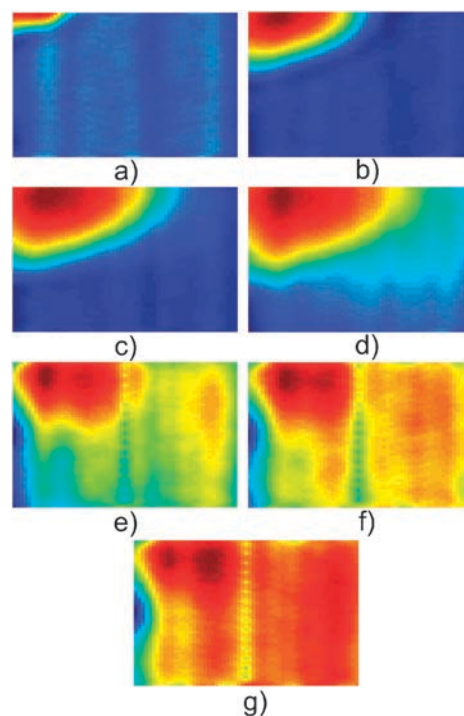
Fig. 5 2D imaging of proton/ion distributions over the 64 × 64-pixel (715.8 × 715.8 µm) ISA of the trigger event in the BZ reaction at time slots of (a) 34 s, (b) 35.7 s, (c) 36.8 s, (d) 37.4 s, (e) 39.7 s, (f) 41.1 s, (g) 43.3 s, red displays the highest and blue the lowest output potential.

It takes approximately 10–14 s for a single propagation wave to travel across the chip, with the size of the ISA being
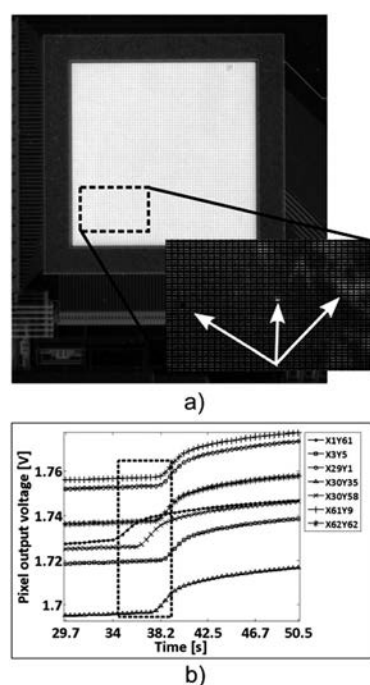
Fig. 6 Corrosive effects (a) of several performed BZ experiments and reaction trigger events and bias variations (b) across the 64 × 64-pixel ISA.

715.8 × 715.8 μm; this results in a propagation velocity of about 3–4 mm min^{-1}, consistent with previous data presented in the literature.[16] Therefore the changes in ionic distributions detected by the ISA can be considered as a propagation wave of the BZ reaction. Fig. 5a presents the measured precision capability of the 64 × 64-pixel ISA based ion imaging technology. It is shown that the ion-camera system could visualize two extremes of pH values at spatial resolution of ∼70 μm that is basically the occupied physical space of 6 consecutive pixels. This fine resolution was observed during all BZ experiments. The pH values between the minimum and maximum ones are recorded by intermediate pixels which enables the monitoring of ion diffusions.

Results of selected pixels have also been analysed to verify the effects of the chemical experiments. Pixels (1;61), (3;5), (30;58), (30;35), (29;1), (62;62) and (61;9), that are located at the four corners and in the middle of the ISA, have been selected for investigations. Large bias variations have prevented the pixels from settling into the same operation points which we attribute to the corrosiveness of the reaction. The selected pixels delivered outmost similarly shaped responses that are illustrated in Fig. 6b. Fig. 6b additionally presents the first trigger event in the response of the selected pixels focusing on the time range of its first and last occurrence. The displayed results support the ones in Fig. 3 showing the same path of reaction with the elevation of the curves in the appropriate sequence.

It is important to notice that the BZ solutions with different concentrations did have a destructive effect on the MET4 (see Fig. 1) top-metal layer. The image Fig. 6a, taken by optical microscope, demonstrates that the MET4 ring around the sensor array has been found transparent after the measurements, showing underlying MET3 metals. The magnified image shows that two pixels were found damaged and a large lighter coloured spot over many sensors implies the development of thinned silicon nitride.

In summary, we show a novel ionic imaging approach with the development of a 64 × 64-pixel ISFET sensor array based ion-camera system. The device is demonstrated to be capable of visualizing the pH flux associated with motion of protons at microscopic level using the well-studied Belousov–Zhabotinsky reaction to image its spontaneous pH fluctuations and ion spread *in situ*. The results presented verify the applicability of the ISA for monitoring dynamics of fluids, implying significant impact on future ISFET imaging for chemical and biological purposes. The deterministic data acquisitions at high temporal resolution of 66 μs per pixel, 17 ms per array provided an approximate 70 μm spatial resolution. Unlike conventional measurement methods, which deliver only bulk information on the reaction, the 64 × 64-pixel ISA successfully captures microscopic localised fluctuations in proton concentrations. We are currently developing acid resistant devices to allow extensive imaging of the BZ reaction under a variety of conditions as well as extending to other dynamic material systems.[17]

Notes and references

1 A. S. Mikhailov and K. Showalter, *Phys. Rep.*, 2006, **425**, 79; G. Biosa, S. Bastianoni and M. Rustici, *Chem.–Eur. J.*, 2006, **12**, 3430.
2 C. Ritchie, G. J. T. Cooper, Y.-F. Song, C. Streb, H. Yin, A. D. C. Parenty, D. A. MacLaren and L. Cronin, *Nat. Chem.*, 2009, **1**, 47.
3 K. Pekala, A. Wiśniewski, R. Jurczakowski, T. Wiśniewski, M. Wojdyga and M. Orlik, *J. Phys. Chem. A*, 2010, **114**, 7903.
4 P. Bergveld, *IEEE Trans. Biomed. Eng.*, 1970, **19**, 70.
5 L. Bousse, N. F. De Rooij and P. Bergveld, *IEEE Trans. Electron Devices*, 1983, **30**, 1263.
6 P. A. Hammond, D. Ali and D. R. S. Cumming, *IEEE Trans. Biomed. Eng.*, 2005, **52**, 687; W. S. W. Zain, T. Prodromakis and C. Toumazou, *IEEE BioCAS*, 2010, 134.
7 A. F. Taylor, V. Gaspar, B. R. Johnson and S. K. Scott, *Phys. Chem. Chem. Phys.*, 1999, **1**, 4595; A. F. Taylor and M. M. Britton, *Chaos*, 2006, **16**, 037103.
8 B. P. Belousov, *Ref. Radiats. Med., 1958, Medgiz, Moscow*, 145, 1959.
9 R. J. Field and M. Burger, *Oscillations and Traveling Waves in Chemical Systems*, John Wiley and Sons, Chichester, 1985.
10 H. Miike and T. Sakurai, *Forma*, 2003, **18**, 197.
11 A. Adamatzky, B. D. L. Costello and T. Asai, *Reaction-Diffusion Computers. Science And Technology*, Elsevier B.V, 2005; A. Kaminaga, V. K. Vanag and I. R. Epstein, *Angew. Chem., Int. Ed.*, 2006, **45**, 3087.
12 R. Yoshida, T. Sakai, Y. Hara, S. Maeda, S. Hashimoto, D. Suzuki and Y. Murase, *J. Controlled Release*, 2009, **140**, 186.
13 S. D. Moss, C. C. Johnson and J. Janata, *IEEE Trans. Biomed. Eng.*, 1978, **BME-25**, 49.
14 A. Garde, J. Aderman and W. Lane, *Sens. Actuators, B*, 1995, **27**, 341.
15 The BZ reaction was prepared according to the the following concentrations: [KBrO$_3$] = 220 mM, [KBr] = 28 mM, [MA] = 64 mM, and [H$_2$SO$_4$] = 200 mM and [Ferroin indicator] = 250 mM. The former four chemicals were mixed creating the *pre-BZ solution* and thereafter ferroin indicator was added to initiate the reaction.
16 R. J. Field, E. Koros and R. M. Noyes, *J. Am. Chem. Soc.*, 1972, **94**, 8649.
17 I. Lagzi1, B. Kowalczyk, D. Wang and B. A. Grzybowski, *Angew. Chem., Int. Ed.*, 2010, **49**, 8616.